Prism-Based Surface Plasmon Resonance for Dual-Parameter Sensing

D. Monzón Hernández, *Member, IEEE*, J. S. Velázquez-González, D. Luna-Moreno, M. Torres-Cisneros, and I. Hernández-Romano

***Abstract*— A simple method to construct a dual-channel in a prism-based surface plasmon resonance sensor for dual-parameter monitoring is proposed. The metal layer (sensing area), attached to the prism, is half-covered with a polymer in order to generate two individual sensing sections. In this paper, eight different sensor structures (prism/metal/polymer) were analyzed. The prisms are made of NSK16 or SF10 glass and coated with gold or silver films. Half section of the metal films is covered with Polydimethylsiloxane (PDMS) or Polymethyl methacrylate. The sensor is based on angle interrogation, the laser beam is aligned to be incident upon the interface of the bare and polymer sections. The resonance conditions are different at each pad, due to the refractive index (RI) mismatch, thus the intensity of the reflected signal presents a pair of well-defined resonance dips in series. The sensitivity of these dips to RI and temperature (T) changes was numerically analyzed. Finally, to demonstrate the feasibility to monitor RI and T, simultaneously, a surface plasmon resonance sensor was constructed using a NSK16 glass prism coated with a thin gold film, which was half-covered with PDMS.**

***Index Terms*— Optical sensors, optical polymers, thin film, plasmon.**

I. Introduction

SURFACE plasmon resonance (SPR) phenomenon is unanimously considered as one of the most sensitive and straightforward techniques to measure the RI of a sample, no matter whether the sample is gaseous, liquid, or solid [1], [2]. The remarkable advantages of the technique have contributed to the successful utilization of this phenomenon in a wide range of chemical and biochemical analysis including detection of pathogens trace in beverages and food [3], measurement of the water content in ethanol-based biofuels [4], or identification of proteins associated with early stage of diseases [5].

The optical excitation of plasmons can be achieved through a coupler (prism, grating, planar or a cylindrical waveguide), coated with a proper thin metal film, or by the direct interaction of light with nanoparticles. The bulky SPR sensors can be credited for the successful exploitation of the phenomenon in commercial and industrial applications. The well-known intrinsic capabilities of the technique, the versatility and adaptability of the setup to fit customer's needs, and the possibility to carry out multi-parameter sensing, have contributed to its success.

The RI of some liquids is highly affected by temperature, this condition could be a serious drawback for highly sensitive RI sensors such as those based on SPR. In order to reduce or compensate the environmental temperature fluctuations, which have been identified as the main source of uncertainty in RI measurement [6]–[8], some authors have proposed the use of dual-channel SPR schemes to generate a self-referencing resonance dip [9]–[13]. In most of such schemes, the outer thin metal film area is divided into two independent and disconnected sections. One of the sections is overcoated with a thin dielectric layer whose RI is higher than that of the samples to be measured. The RI mismatch between the two sections produce a pair of resonance dips in series. The first one, at a shorter wavelength (λ_S), to monitor the RI changes and the reference dip, at a larger wavelength (λ_R), generated by the dielectric overlayer. Recently, in order to deal with the adverse effects of temperature fluctuations, novel SPR sensor schemes for the simultaneous measurement of RI and T have been proposed [14]–[19]. However, in the case of the prism-based SPR sensors the experimental setup is complicated and mechanically unstable due to the presence of several extra bulky elements [14], [15]. In the fiber-based RI SPR sensors the T changes are monitored with an extra fiber device such as Fabry-Perot cavity [16] or Bragg grating [17], which increases the length of the sensor head. The temperature sensitivities achieved with those schemes are far below the 0.5 nm/°C. Lately, a pair of compact dual-channel fiber-based sensors, where RI and T changes were monitored by a pair of SPR dips, have been reported [18], [19]. In [18], Weng *et al.* proposed the creation of double-side polished surfaces in the fiber, coated with gold and silver, respectively, to produce two orthogonally polarized plasmons. The sensor head was compact but the sensitivities, to RI as well as T, were similar to that reported by conventional methods, moreover the fabrication technique was quite demanding. In [19],

Manuscript received November 27, 2017; revised February 23, 2018; accepted March 17, 2018. Date of publication March 21, 2018; date of current version April 23, 2018. This work was supported by the Consejo Nacional de Ciencia y Tecnología (CONACyT) from México under the CIENCIA BÁSICA Project 257046. The work of J. S. Velázquez-González was supported by CONACyT through a Post-Doctoral Scholarship. The work of I. Hernández-Romano was supported by the project: "Cátedras CONACYT 2015." The associate editor coordinating the review of this paper and approving it for publication was Dr. Ioannis Raptis. *(Corresponding author: D. Monzón Hernández.)*

D. M. Hernández, J. S. Velázquez-González, and D. Luna-Moreno are with the Centro de Investigaciones en Óptica A. C., León 37150, México (e-mail: dmonzon@cio.mx; jsvelazquezg@gmail.com; jsvelazquezg@cio.mx; dluna@cio.mx).

M. Torres-Cisneros is with the Electronics Department, DICIS, University of Guanajuato, Guanajuato 36885, México (e-mail: torres.cisneros@ugto.mx).

I. Hernández-Romano is with the CONACYT-Electronics Department, University of Guanajuato, Guanajuato 36885, México (e-mail: heriromano@gmail.com).

Digital Object Identifier 10.1109/JSEN.2018.2818064

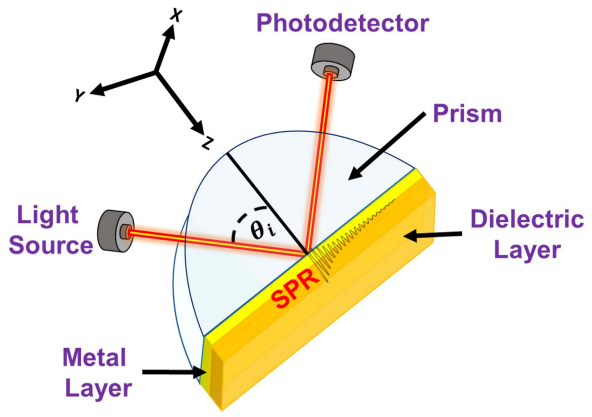

Fig. 1. Kretschmann configuration for SPR excitation.

we recently reported a SPR sensor based on a hetero-core fiber structure where half of the single-mode fiber, coated with a gold layer of 30 nm, was covered with a polymer. The wavelength spectra exhibited a pair of resonance dips, where one of them was exclusively sensitive to temperature changes. This sensor is easy to fabricate, highly stable, and compact since it is only 5 mm long. This simple idea for simultaneous measurement of RI and T can be replicated in bulky SPR scheme.

In this work, we propose a simple method to construct a dual-channel SPR sensor in Kretschmann configuration, by covering half of the metal layer, attached to the prism, with a polymer. When laser beam struck at the metal-bare – polymer interface, a pair of plasmon waves were excited. The reflected intensity exhibited a pair of SPR loss dips, located at different incident angles accordingly to the RI of the external medium and polymer. The metal-bare section was sensitive to RI changes of the external medium while the polymer-pad was used for monitoring temperature changes. The dual-pad SPR sensors for the simultaneous measurement of RI and T are theoretically analyzed, and the structure with better performance was fabricated and tested as the experimental proof of the numerical analysis.

II. Principle of SPR in Krestchmann Configuration

Surface plasmon waves (SPW's) are charge-density oscillations at the interface of a metal and a dielectric, which can be excited by electrons [20], [21], phonons [22] and photons [23]. In the case of photons, the SPW's are excited when the phase matching conditions between the optical and plasmon wave vector are satisfied. In Krestchmann configuration the energy of the incoming light is coupled to the plasmon, via the evanescent wave generated by the total internal reflection [23]–[26], as shown in Fig. 1.

The angle interrogation technique consists in measuring the intensity of the reflected p-polarized beam with a photodetector while the incident angle of the beam is changing, see Fig. 1. A simulation of this process was carried out to evaluate the Reflectance (Rp) using the multi-layer (N-layer) model described in [27] and [28]. This model defines a stratified medium as a stack of thin homogeneous films (N-layer) of thickness d_k, dielectric constant ε_k, permeability μ_k, and refractive index n_k of the k-layer along the Z-direction. In addition, this model assumes that all the layers are uniform, isotropic, and non-magnetic where the tangential components of the electric and magnetic fields at the first boundary $Z = Z_1 = 0$ are related to those at the final boundary $Z = Z_{N-1}$ by:

$$\begin{bmatrix} U_1 \\ V_1 \end{bmatrix} = M \begin{bmatrix} U_{N-1} \\ V_{N-1} \end{bmatrix}. \tag{1}$$

In equation (1), $U_1(V_1)$, and $U_{N-1}(V_{N-1})$ are the tangential components of electric (magnetic) field at the boundary of the first and *(N-1)-th* layer, respectively. Here, M is known as the characteristic matrix of the combined structured, and it is mathematically expressed as follows:

$$M = \prod_{k=2}^{N-1} M_k = \prod_{k=2}^{N-1} \begin{bmatrix} \cos\beta_k & \frac{-isin\beta_k}{q_k} \\ -iq_k sin\beta_k & \cos\beta_k \end{bmatrix}, \tag{2}$$

with, $q_k = \left(\sqrt{\varepsilon_k - n_1^2 sin^2\theta_1}\right)/\varepsilon_k$ and $\beta_k = (2\pi d_k/\lambda) \cdot \sqrt{\varepsilon_k - n_1^2 sin^2\theta_1}$, where n_1 represents the RI of the incident medium (prism); λ and θ_1 are the wavelength of the p-polarized laser beam and the incident angle measured respect to the normal at the prism-metal layer interface, respectively. While, β_k is the propagation constant of the light at the k_{th} layer. Finally, the amplitude of the reflected wave (r_p) and R_p are given by:

$$r_p = \frac{(M_{11} + M_{12}q_N)\,q_1 - (M_{21} + M_{22}q_N)}{(M_{11} + M_{12}q_N)\,q_1 + (M_{21} + M_{22}q_N)} \text{ and } R_p = |r_p|^2. \tag{3}$$

III. The Structure of the SPR Sensor

The basic structure of the SPR sensor is depicted in Fig. 1, consisting of a prism, a thin metal film, and an external medium. In order to generate a dual-channel SPR sensor, i.e. two SPR dips, the thin metal film is half-covered with a polymer. The incident light beam is aligned to strike at the boundary between the metal-bare and the polymer-pad producing two plasmon waves. The reflected signal exhibits a pair of resonance dips at angles labeled as θ_{Bare} and $\theta_{Polymer}$, whose relative position depends on the RI of the sample (n_{sample}) and polymer ($n_{polymer}$), respectively. It is also assumed that the polymer layer is thick enough (5 mm approximately) to isolate the polymer plasmon wave from the influence of the n_{sample}. The polymer resonance angle ($\theta_{Polymer}$) can be used as a reference angle to detect, and eventually compensate, external perturbations that could lead to errors during the RI measurement. The structure of the proposed sensor is shown in Fig. 2.

IV. Theoretical Analysis of the Dual-Pad SPR Sensor

Assuming that laser beam is incident exactly at the middle of the interface between the metal-bare and the polymer-pad, each section of the external medium equally contributes to the

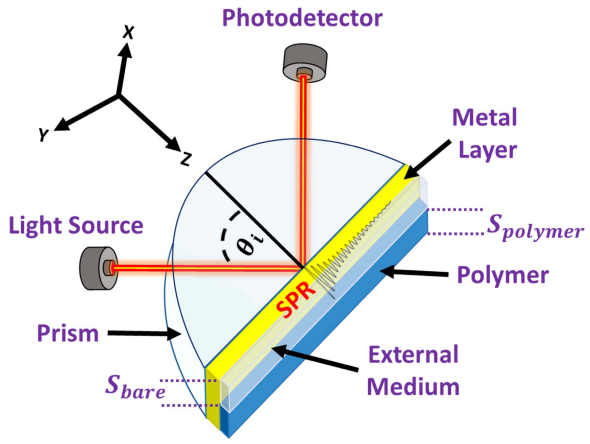

Fig. 2. The structure of the prism-based double-pad SPR sensor.

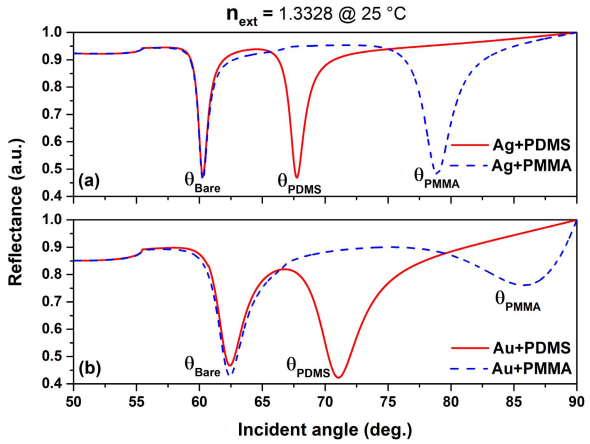

Fig. 3. Theoretical reflectance in a NSK16 prism coated with (a) silver and (b) gold.

final reflectivity of the signal and this can be described as follows,

$$R_{dual-pad} = \frac{1}{2}\left|r_p\left(Bare\right)\right|^2 + \frac{1}{2}\left|r_p\left(Polymer\right)\right|^2. \quad (4)$$

A numerical simulation of the reflected intensity of the dual-pad SPR was accomplished by following the steps described in the *N-layer* model [27], [28] and Eq. (4). In the analysis we assumed that the emission of the laser used is centered at a wavelength of 632.8 nm, two types of glasses (NSK16 and SF10), metals (silver and gold) and polymers (PDMS and PMMA) were considered. The refractive indexes (at 25 °C) are $n_{NSK16} = 1.6183$ and $n_{SF10} = 1.7232$ [29]; $n_{Ag} = 0.06656 + i\ 4.0452$ and $n_{Au} = 0.16195 + i\ 3.20991$ [30]; $n_{PDMS} = 1.4118$ [30], and $n_{PMMA} = 1.4889$ [31]; and $n_{H20} = 1.3328$. It is worth mentioning that the sensing area (metal layer) is equally divided into two sections: sample and polymer.

The reflectance of the NSK16 prism coated with 50nm of silver layer is shown in the graphs of Fig. 3 (a); when half of the metal layer is covered with PDMS and the rest with water (continuous red line), the angle separation between the dips is 8°. The separation is two times larger (19°) when PDMS is substituted by PMMA (dashed blue line). When the

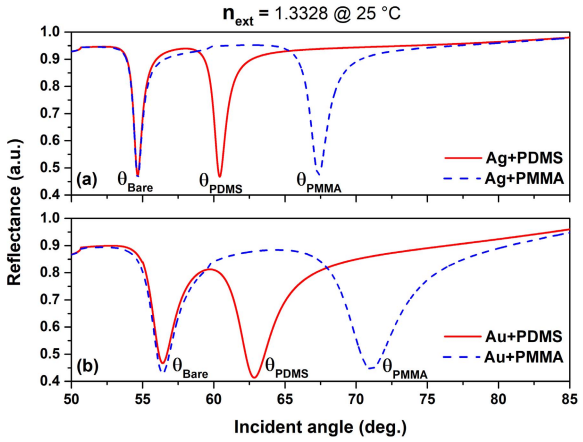

Fig. 4. Theoretical reflectance in a SF10 prism coated with (a) silver and (b) gold.

NSK16 prism is coated with a gold layer and half-covered with PDMS (continuous red line in Fig. 3 (b)), the angle separation between the θ_{Bare} and θ_{PDMS} is approximately 9°. PMMA produces a notorious deformation in the second SPR dip (dashed blue line of Fig. 3(b)), due to its high RI. Clearly, the high RI of PMMA makes it not suitable for this structure.

The SPR reflectance of a prism fabricated with SF10 glass, whose RI is higher than NSK16, coated with silver or gold film and half-coated with PDMS (continuous red line) or PMMA (dashed blue line), are shown in Fig. 4 (a) and (b). The angle difference between θ_{Bare} and $\theta_{Polymer}$ is 6° and 12° in the case of silver-PDMS and silver-PMMA, respectively; and it is 8° and 15° for gold-PDMS and gold-PMMA, respectively. In all cases the dips are well-behaved.

As it is evident from Fig. 3 and Fig. 4, one of the dips (θ_{Bare}) is generated by the metal-bare section whose resonance angel is tuned by n_{sample}. The other dip ($\theta_{Polymer}$) is produced by the polymer and the resonance angle ($\theta_{PDMS/PMMA}$) depends on the RI of the polymer used. The SPR dips generated by the thin silver film partially covered with PMMA are sharper since the real and imaginary part of the dielectric constant of silver are smaller than that of the gold [32]. The separation between θ_{bare} and $\theta_{polymer}$ increases due to the increment of the RI difference between water and PMMA. It is important to notice that the reduction of the separation between resonance dips (bare and polymer) tends to distort its shape.

The effect of the external RI change in the response of the SPR sensor was analyzed. The SPR reflectance of the NSK16/silver/PMMA and SF10/gold/PMMA are shown in Fig. 5 (a) and (b), respectively. The resonance angle $\theta_{Polymer}$ is unaltered due to the thickness of the polymer considered in the analysis. The shape of the dips is not altered due to its large separation. The RI dynamic range (DR) of the NSK16/silver/PMMA is larger due to the large dips separation, also its sensitivity is bigger than SF10/gold/PMMA, as can be seen in graphs of Fig. 6. It is possible to conclude that the increment (decrement) of the RI of the glass prism increases (decreases) the DR but decreases (increases) the sensitivity of

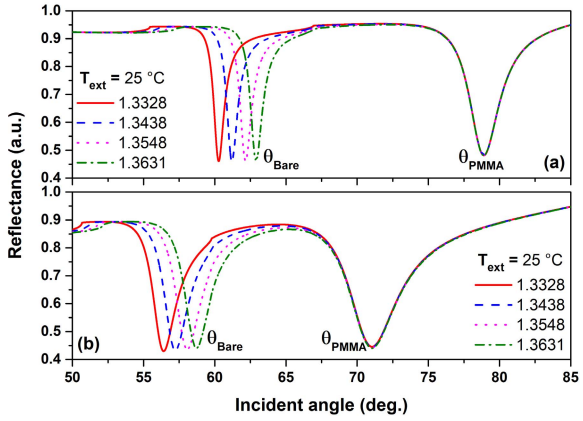

Fig. 5. Theoretical reflectance of (a) NSK16 prism coated with silver and (b) SF10 prism coated with gold.

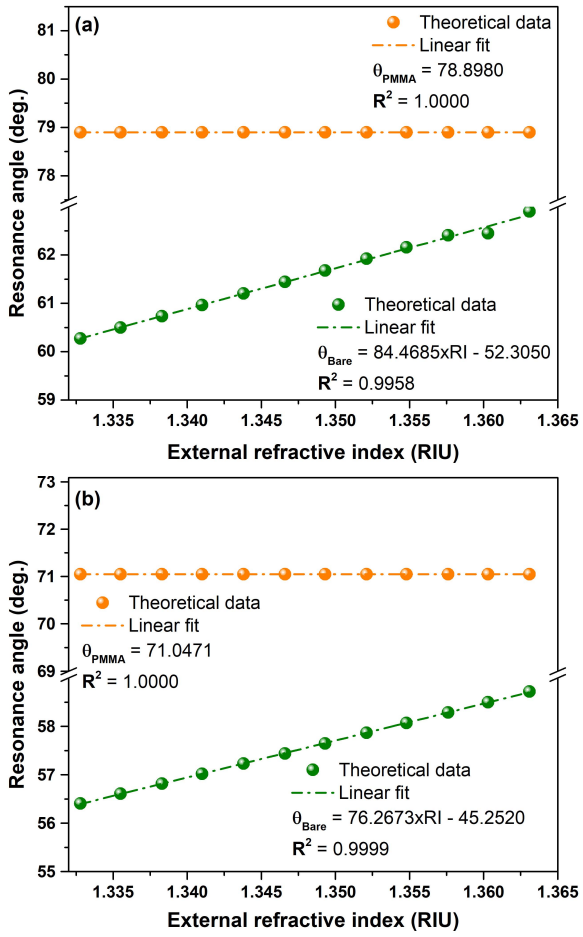

Fig. 6. Theoretical RI sensitivity of (a) the NSK16 prism coated with silver and (b) SF10 prism coated with gold.

the SPR RI sensor. Besides the SPR dip of the bare section is sensitive to the RI and T changes [6]–[8], but the dip generated by the polymer section is exclusively sensitive to the T of the surrounding medium.

Although the SPR signal of the silver-coated prisms exhibits sharper dips, the gold films seem to be more appropriate for a liquid RI sensor. The reason for this is that the silver films

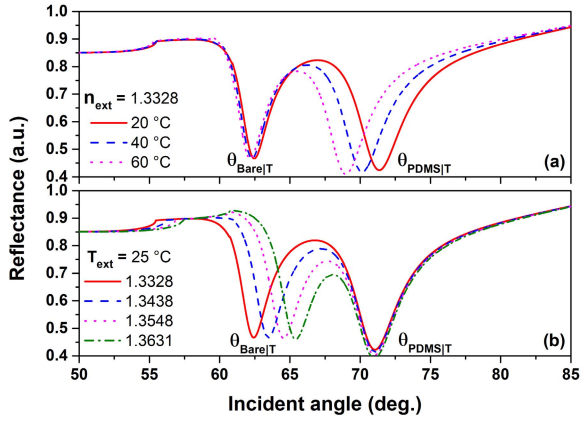

Fig. 7. Theoretical reflectance of NSK16 prism coated with gold layer that was half-covered with PDMS and covered with water (a) at three different temperatures and (b) four different RI at 25°C.

could present a low chemical stability and are prone to oxidation [33]. Regarding the temperature sensitivity, the PDMS, whose thermo-optic coefficient (TOC) (-4.66×10^{-4}/°C [35]) is higher than that of the PMMA (-1.3×10^{-4}/°C [34]), is a better alternative as covering polymer. The structure that shows the better performance, for the simultaneous measurement of RI and T, consists of a NSK16 prism coated with a gold film and half-covered with PDMS. The effect of the temperature changes in the theoretical response of the SPR sensor is shown in Fig. 7 (a). It is assumed that the external medium is water with a RI of 1.3328 at 25 °C (continuous red line). When temperature is increasing the RI of the water and the PDMS is decreasing, and both resonance dips are moving to smaller angles. It is important to notice that the displacement of $\theta_{Polymer}$ is approximately eight times larger than θ_{Bare}. When the external RI increases and the temperature is fixed at 25°C, the θ_{Bare} shifts towards greater angles as shown in Fig. 7 (b). As the separation between the dips (θ_{Bare} and $\theta_{Polymer}$) is reduced, the shape of the dips is distorted.

The response of the proposed sensor to T and RI changes is summarized in Fig. 8 (a) and (b), respectively. The temperature sensitivities of bare section (S_{T-Bare}) and polymer-pad ($S_{T-Polymer}$) are −0.0074 and -0.0596 deg/°C, respectively. The RI sensitivities of the bare ($S_{RI-Bare}$) and polymer ($S_{RI-Polymer}$) are 98.6797 and 0 deg/RIU, respectively. Fig. 8 (b) shows that the RI sensitivity of the polymer section ($S_{RI-polymer}$) is constant; thus, that section is insensitive to RI changes. It is worth mentioning that in order to ensure the insensitivity to RI changes, the thickness of the polymer layer needs to be higher than 500 nm. On the other hand, the changes of RI and T produce variations in the resonance angles (θ_{Bare} and $\theta_{Polymer}$), that can be numerically expressed by the following set of equations:

$$\begin{bmatrix} \theta_{Bare} \\ \theta_{Polymer} \end{bmatrix} = \begin{bmatrix} -0.0074 & 98.6797 \\ -0.0596 & 0 \end{bmatrix} \begin{bmatrix} \Delta T \\ \Delta n \end{bmatrix}, \quad (5)$$

where, the sensing matrix can be expressed as:

$$\begin{bmatrix} \Delta T \\ \Delta n \end{bmatrix} = \frac{1}{5.8813} \begin{bmatrix} 0 & -98.6797 \\ 0.0596 & -0.0074 \end{bmatrix} \begin{bmatrix} \theta_{Bare} \\ \theta_{Polymer} \end{bmatrix}. \quad (6)$$

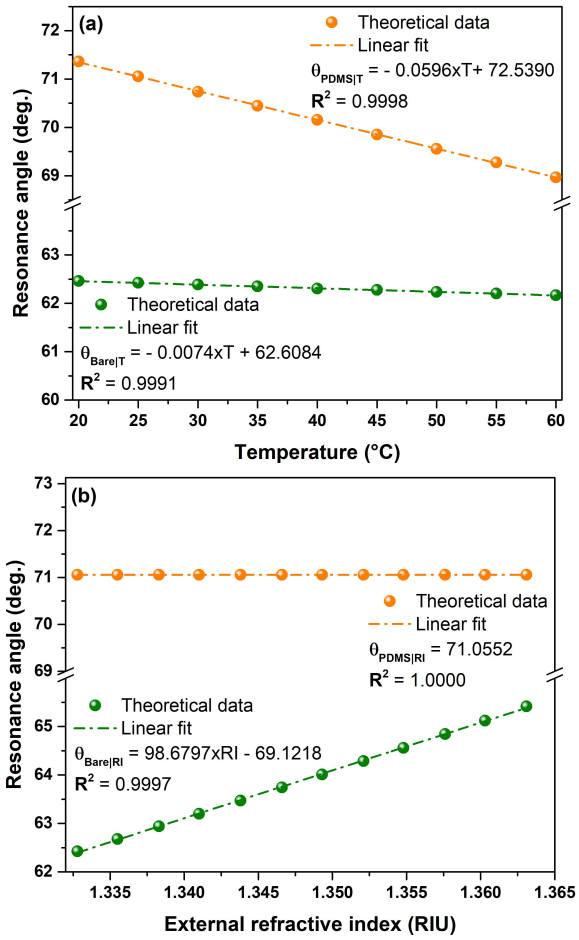

Fig. 8. Theoretical resonance angle of the dips for: (a) different temperatures, assuming that sensing section is covered with water, and (b) different RI, assuming that the temperature is constant at 25 °C.

The angles (θ_{Bare} and $\theta_{Polymer}$), the temperature changes (ΔT) and the RI changes (Δn) are in units of degrees, degrees Celsius, and RIU (Refractive Index Units), respectively. Consequently, the total RI change can be expressed now as:

$$\Delta n = 10.1337 \times 10^{-3}\theta_{Bare} + 0.0750 \times 10^{-3}\Delta T. \quad (7)$$

The changes of θ_{Bare} are the result of the combined effect of the RI and T of the external medium. The second term of Eq. (7) represents the uncertainty on the measurement and it compensates the thermal perturbation on the RI of the external medium. The presented theoretical SPR analysis predicts that it is feasible to measure the RI and T simultaneously using the dual-pad sensor proposed.

In the previous analysis we assumed that both sensing sections are equally irradiated by the incident beam; however, in a real experiment this position can be altered by mechanical instabilities produced by relaxation of the different elements of the experimental setup or due to external vibrations. In Fig. 9, it is shown that theoretical reflectance when the incident beam is perfectly centered (50-50 continuous red line) at the interface air-PDMS, when it is misaligned by 80% and the intensity strikes at the PDMS-pad (80-20 dotted green line) and when 80% of the intensity strikes at the bare section

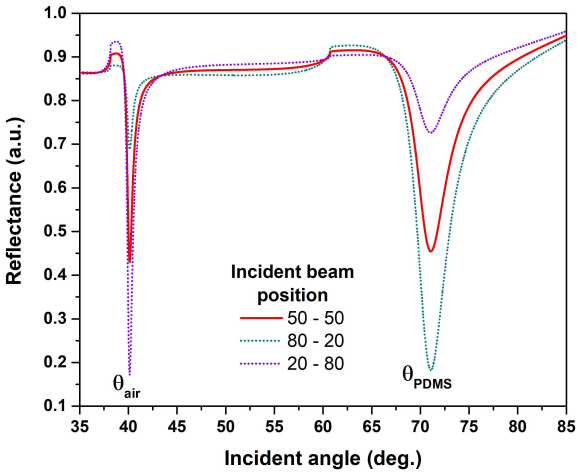

Fig. 9. Theoretical reflectance for three different positions of the incident beam at the interface air-PDMS.

surrounded by air (20-80 dotted purple line). As the beam is displaced from the central positon of the interface the intensity of light increases and the loss level of the dip increases. The displacement of the beam respect to its initial position can be perfectly detected by analyzing the changes in the dip losses.

V. Experimental Results

An experimental demonstration of the previous numerical simulation was carried out by using gold and PDMS such as thin metal film and polymer coating, respectively. The gold film was selected instead of silver due to its chemical properties such as stability and non-oxidation, whilst the PDMS polymer was chosen rather than PMMA due to its high TOC; moreover, it protects the gold film against dust and scratches.

The structure consisting of a semi-cylindrical prism made of NSK16 glass coated with a 50 nm gold-layer, which was half-covered with PMDS. The fabrication of the prism as well as the deposition of the thin metal film layer were carried out in our optical workshop facilities, the PDMS was prepared in our laboratory. The fabrication of each element and the final structure of the experimental setup were discussed in detail in [30] and [36]. After thin film deposition, a glass cuvette was attached to the flat surface of the gold-coated prism. Then PDMS was poured to cover half of the total volume of the container and cured by heating it up at 60°C for 4 hours [37]. After curing, the beam was aligned to strike at the air-PDMS interface. The experimental reflectance is shown in Fig. 10, where a pair of almost symmetrical dips can be noticed (continuous red line). The position of the laser beam was displaced from air-PDMS interface producing a change in the dips losses. It is important to notice the similarities with the theoretical curves shown in Fig. 9.

Part of the remaining volume of the cuvette was filled with distilled water. Three sections can be perfectly distinguished: air at the top, water at the middle, and the PDMS at the bottom. A schematic drawing of the final structure is shown in Fig. 11. The vertical position of the prism was varied with respect to the incident beam in order to obtain the SPR signal of

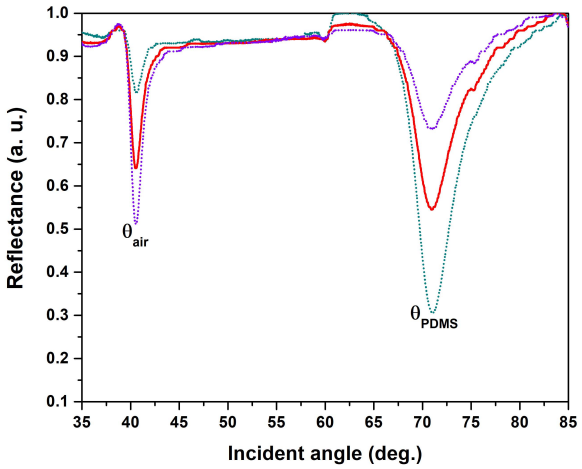

Fig. 10. Experimental SPR reflectance for three different positions of the incident beam respect to the air-PDMS interface.

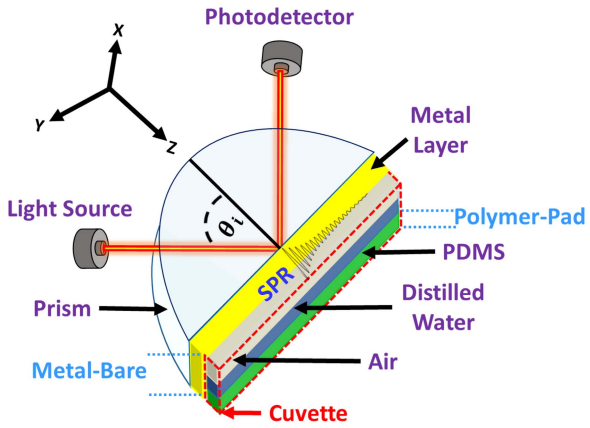

Fig. 11. A schematic drawing of the proposed sensor.

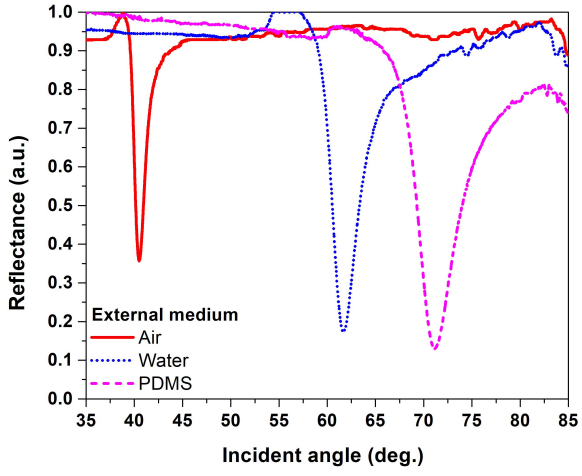

Fig. 12. Experimental reflectance of the SPR sensor when external medium is air (continuous red line), distilled water (dotted blue line), and PDMS (dashed magenta line).

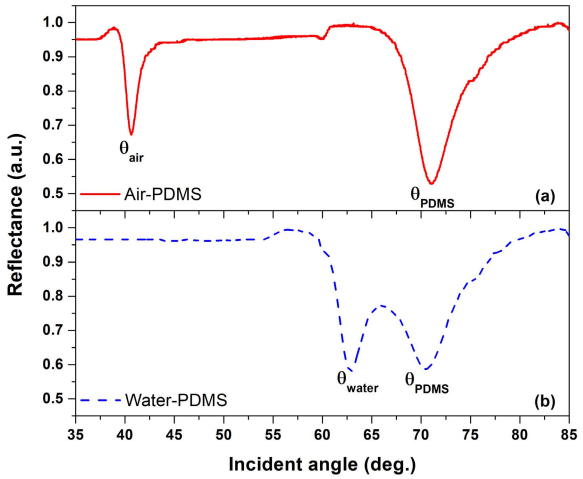

Fig. 13. Experimental reflectance of the SPR sensor when beam is incident at the interface (a) air-PDMS and (b) water-PDMS.

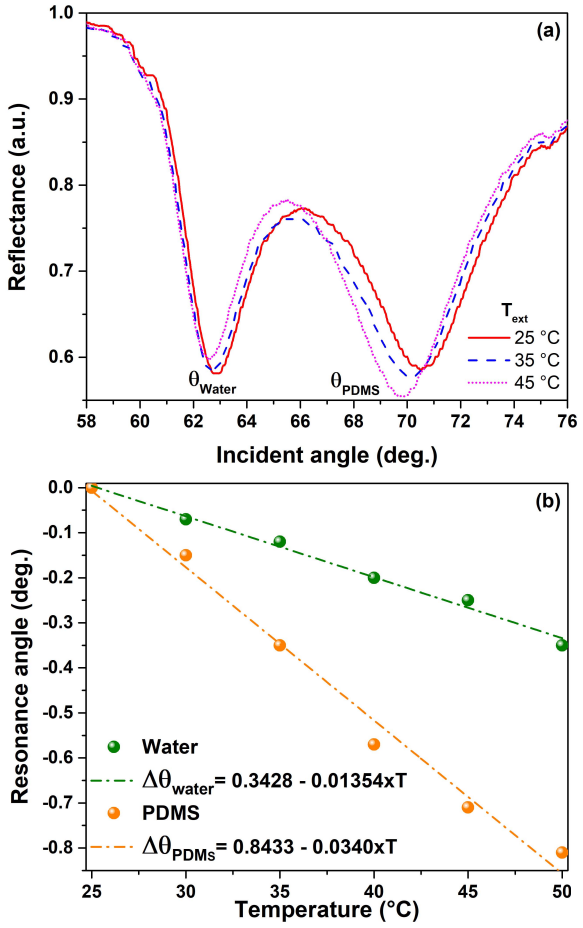

Fig. 14. Experimental SPR reflectance of the sensor: (a) at three different temperatures when laser beam is incident at the interface water-PDMS, and (b) the displacement of the resonance angle at different temperatures.

three independent mediums: air, distilled water and PDMS. The vertical displacement was achieved by setting the prism onto a translation stage that allows us to move it to different positions, without the need of changing the detector's place.

Fig. 12 shows the experimental reflectance for three external media; air (continuous red line), distilled water (dotted blue line), and PDMS (dashed magenta line). The resonance angles of the dips for air, distilled water, and PDMS (whose RI at 632.8 nm are 1.0002, 1.3328, and 1.4118, respectively) were 40°, 61.7°, and 71.1°, respectively. The width and the depth of the dips increases as the RI of the substance increases. When the upper part of the container is filled with water, the changes in the external RI of the metal-bare section from 1.0002 (air)

to 1.3328 (water) produced a displacement of the first dip from a resonance angle of 40° to 62.1°, as can be observed in Fig. 13 (a) and (b). Besides, in Fig. 13 (b), it is evident that the proximity of the resonance dips generates a mutual perturbation affecting the shape of the peaks.

In order to analyze the temperature sensitivity of the dual-pad SPR sensor, the container was heated by means of an electrical resistance attached to the external wall. A calibrated thermocouple was previously inserted in the PDMS to measure the temperature. The experimental reflectance for three different temperatures is shown in Fig. 14 (a). Since water and PDMS possess a negative TOC the resonance dips shifted to smaller angles while the temperature was increased, as can be seen in the Fig. 14 (b). The total change of the resonance angle was different for both dips because the TOC of the materials was different.

The variation of experimental resonance angle as a function of the temperature can be approximated by a linear fit, both sensitivities are negative. Due to the higher TOC of PDMS the sensitivity of the polymer resonance dip (−0.034 deg/°C) was two times larger than that of the water (−0.0135 deg/°C). The resolution of the mechanical mounts was 0.01°; thus, the temperature resolution of the PDMS dip was 0.3°C. The calculated sensitivity of PDMS is slightly higher than that obtained experimentally.

VI. Conclusion

A novel and simple method to generate a dual-channel prism-based SPR sensor was proposed, theoretically analyzed and experimentally demonstrated. In our study we analyzed the RI and T sensitivities of several structures. One of these structures was constructed and tested to demonstrate the feasibility to measure the RI and T of a liquid sample simultaneously. The SPR sensor structure was composed by a prism coated with a thin metal film and a dielectric or external medium. We proposed to cover half area of the metal layer (sensing area) with a polymer to generate two adjacent sensing sections. When the laser beam was incident at the metal-bare – polymer interface, the intensity was divided between these two sections producing a pair of independent plasmon resonances. The sensor was based on angle interrogation of SPR, thus the reflected intensity presented a pair of well-defined resonance dips in series. One of them was generated at the metal-bare section and was still used to measure the RI of a liquid samples in contact with the metal. The other dip was directly related to the RI of the polymer that is in contact with the thin metal film, although the polymer was in contact with the liquid, the polymer resonance dip was independent of the changes of the sample RI as a consequence of its thickness. Finally, the polymer dip can be used as a reference to compensate undesirable perturbations, or for measuring another property of the liquid.

Acknowledgment

The authors are grateful to the Dirección de Investigación, the mechanical and optical workshop of the Centro de Investigaciones en Óptica A. C. for their support and assistance in the fabrication of some samples.

References

[1] J. Homola, S. S. Yee, and G. Gauglitz, "Surface plasmon resonance sensors: Review," *Sens. Actuators B, Chem.*, vol. 54, nos. 1–2, pp. 3–15, 1999.

[2] M. Piliarik and J. Homola, "Surface plasmon resonance (SPR) sensors: Approaching their limits?" *Opt. Exp.*, vol. 17, no. 19, pp. 16505–16517, 2009.

[3] V. Koubová *et al.*, "Detection of foodborne pathogens using surface plasmon resonance biosensors," *Sens. Actuators B, Chem.*, vol. 74, nos. 1–3, pp. 100–105, 2001.

[4] S. K. Srivastava, R. Verma, and B. D. Banshi, "Surface plasmon resonance based fiber optic sensor for the detection of low water content in ethanol," *Sens. Actuators B, Chem.*, vol. 153, no. 1, pp. 194–198, Mar. 2011.

[5] S. Kumbhat, K. Sharma, R. Gehlot, A. Solanki, and V. Joshi, "Surface plasmon resonance based immunosensor for serological diagnosis of dengue virus infection," *J. Pharmaceutical Biomed. Anal.*, vol. 52, no. 2, pp. 255–259, 2010.

[6] H.-P. Chiang, Y.-C. Wang, P. T. Leung, and W. S. Tse, "A theoretical model for the temperature-dependent sensitivity of the optical sensor based on surface plasmon resonance," *Opt. Commun.*, vol. 188, nos. 5–6, pp. 283–289, 2001.

[7] Ş. K. Özdemir and G. Turhan-Sayan, "Temperature effects on surface plasmon resonance: Design considerations for an optical temperature sensor," *J. Lightw. Technol.*, vol. 21, no. 3, pp. 805–814, Mar. 2003.

[8] C. S. Moreira, A. M. N. Lima, H. Neff, and C. Thirstrup, "Temperature-dependent sensitivity of surface plasmon resonance sensors at the gold—water interface," *Sens. Actuators B, Chem.*, vol. 134, no. 2, pp. 854–862, 2008.

[9] G. G. Nenninger, J. B. Clendenning, C. E. Furlong, and S. S. Yee, "Reference-compensated biosensing using a dual-channel surface plasmon resonance sensor system based on a planar lightpipe configuration," *Sens. Actuators B, Chem.*, vol. 51, nos. 1–3, pp. 38–45, 1998.

[10] J. Homola, H. B. Lu, and S. S. Yee, "Dual-channel surface plasmon resonance sensor with spectral discrimination of sensing channels using dielectric overlayer," *Electron. Lett.*, vol. 35, no. 13, pp. 1105–1106, Jun. 1999.

[11] Q. Zou, N. Menegazzo, and K. S. Booksh, "Development and investigation of a dual-pad in-channel referencing surface plasmon resonance sensor," *Anal. Chem.*, vol. 84, no. 18, pp. 7891–7898, Sep. 2012.

[12] C. Fallauto, Y. Liu, G. Perrone, and A. Vallan, "Compensated surface plasmon resonance sensor for long-term monitoring applications," *IEEE Trans. Instrum. Meas.*, vol. 63, no. 5, pp. 1287–1292, May 2014.

[13] S. K. Srivastava, R. Verma, and B. D. Gupta, "Theoretical modeling of a self-referenced dual mode SPR sensor utilizing indium tin oxide film," *Opt. Commun.*, vol. 369, pp. 131–137, Jun. 2016.

[14] F. Xiao, D. Michel, G. Li, A. Xu, and K. Alameh, "Simultaneous measurement of refractive index and temperature based on surface plasmon resonance sensors," *J. Lightw. Technol.*, vol. 32, no. 21, pp. 4169–4173, Nov. 1, 2014.

[15] W. Luo *et al.*, "Dual-angle technique for simultaneous measurement of refractive index and temperature based on a surface plasmon resonance sensor," *Opt. Exp.*, vol. 25, no. 11, pp. 12733–12742, 2017.

[16] S. Chen, Y. Liu, Q. Liu, and W. Peng, "Temperature-compensating fiber-optic surface plasmon resonance biosensor," *IEEE Photon. Technol. Lett.*, vol. 28, no. 2, pp. 213–216, Jan. 15, 2016.

[17] T. Hu, Y. Zhao, and A.-N. Song, "Fiber optic SPR sensor for refractive index and temperature measurement based on MMF-FBG-MMF structure," *Sens. Actuators B, Chem.*, vol. 237, pp. 521–525, Dec. 2016.

[18] S. Weng, L. Pei, C. Liu, J. Wang, J. Li, and T. Ning, "Double-side polished fiber SPR sensor for simultaneous temperature and refractive index measurement," *IEEE Photon. Technol. Lett.*, vol. 28, no. 18, pp. 1916–1919, Sep. 15, 2016.

[19] J. S. Velázquez-Gonzélez, D. Monzán-Hernéndez, D. Moreno-Hernández, F. Martínez-Piñén, and I. Hernéndez-Romano, "Simultaneous measurement of refractive index and temperature using a SPR-based fiber optic sensor," *Sens. Actuators B, Chem.*, vol. 242, pp. 912–920, Apr. 2017.

[20] T. Wang, E. Boer-Duchemin, Y. Zhang, G. Comtet, and G. Dujardin, "Excitation of propagating surface plasmons with a scanning tunnelling microscope," *Nanotechnol.*, vol. 22, no. 17, p. 175201, 2011.

[21] P. Bharadwaj, A. Bouhelier, and L. Novotny, "Electrical excitation of surface plasmons," *Phys. Rev. Lett.*, vol. 106, no. 22, p. 226802, 2011.

[22] B. Diaconescu *et al.*, "Low-energy acoustic plasmons at metal surfaces," *Nature*, vol. 448, pp. 57–59, Jul. 2007.

[23] H. Raether, *Surface Plasmons on Smooth and Rough Surfaces and on Gratings* (Springer Tracts in Modern Physics), vol. 111. Berlin, Germany: Springer-Verlag, 1988.
[24] E. Kretschmann and H. Raether, "Notizen: Radiative decay of non radiative surface plasmons excited by light," *Zeitschrift Naturforschung A*, vol. 23, no. 12, pp. 2135–2136, 1968.
[25] S. Herminghaus and P. Leiderer, "Surface plasmon enhanced transient thermoreflectance," *Appl. Phys. A, Solids Surf.*, vol. 51, no. 4, pp. 350–353, 1990.
[26] B. Liedberg, C. Nylander, and I. Lunström, "Surface plasmon resonance for gas detection and biosensing," *Sens. Actuators*, vol. 4, pp. 299–304, Jan. 1983.
[27] F. Abelès, "Recherches sur la propagation des ondes électromagnétiques sinusoïdales dans les milieux stratifiés," *Ann. Phys.*, vol. 12, no. 5, pp. 596–640, 1950.
[28] Y. Yuan, L. Ding, and Z. Guo, "Numerical investigation for SPR-based optical fiber sensor," *Sens. Actuators B, Chem.*, vol. 157, no. 1, pp. 240–245, 2011.
[29] *Schott 2017 Optical Glass Data Sheet*. Accessed Sep. 21, 2017. [Online]. Available: http://www.schott.com/d/advanced_optics/ac85c64c-60a0-4113-a9df-23ee1be20428/1.1/schott-optical-glass-collection-datasheets-english-17012017.pdf
[30] Y. M. Espinosa-Sánchez, D. Luna-Moreno, M. Rodríguez-Delgado, and A. Saánchez-Álvarez, "Determination of optical parameters of organic and inorganic thin films using both surface plasmon resonance and Abelès-Brewster methods," *Optik-Int. J. Light Electron Opt.*, vol. 142, pp. 426–435, Aug. 2017.
[31] J. W. Gooch, Ed., *Encyclopedic Dictionary of Polymers*, 2nd ed. Atlanta, GA, USA: Springer, 2011.
[32] Y. S. Dwivedi, A. K. Sharma, and B. D. Gupta, "Influence of skew rays on the sensitivity and signal-to-noise ratio of a fiber-optic surface-plasmon-resonance sensor: A theoretical study," *Appl. Opt.*, vol. 46, no. 21, pp. 4563–4569, 2007.
[33] S. K. Mishra and B. D. Gupta, "Surface plasmon resonance based fiber optic pH sensor utilizing Ag/ITO/Al/hydrogel layers," *Analyst*, vol. 138, no. 9, pp. 2640–2646, 2013.
[34] Z. Zhang, P. Zhao, P. Lin, and F. Sun, "Thermo-optic coefficients of polymers for optical waveguide applications," *Polymer*, vol. 47, no. 14, pp. 4893–4896, Jun. 2006.
[35] C. Moreno-Hernández, D. Monzón-Hernéndez, I. Hernéndez-Romano, and J. Villatoro, "Single tapered fiber tip for simultaneous measurements of thickness, refractive index and distance to a sample," *Opt. Exp.*, vol. 23, no. 17, pp. 22141–22148, 2015.
[36] Y. M. Espinosa-Sánchez, D. Luna-Moreno, and D. Monzón-Hernández, "Detection of aromatic compounds in tequila through the use of surface plasmon resonance," *App. Opt.*, vol. 54, no. 14, pp. 4439–4446, 2015.
[37] J. S. Velázquez-González, D. Monzón-Hernández, F. Martínez-Piñén, D. A. May-Arrioja, and I. Hernández-Romano, "Surface plasmon resonance-based optical fiber embedded in PDMS for temperature sensing," *IEEE J. Sel. Topics Quantum Electron.*, vol. 23, no. 2, pp. 126–131, Mar./Apr. 2017.

D. Monzón Hernández received the Ph.D. degree from the Universidad of Guanajuato, Mexico, in 1999. Since 2002, he has been a Research Fellow with the Centro de Investigaciones en Óptica A. C., where he is currently involved in the design and fabrication of optical fiber devices and sensors. His research interest includes optofluidics and biosensors.

J. S. Velázquez-González received the B.Eng. degree in communications and electronics and the M.Sc. degree in electronics engineering from the Instituto Politécnico Nacional (IPN–ESIME Zac. and SEPI-ESIME Zac.), in 2008 and 2011, respectively, and the Ph.D. degree from IPN-CIITEC in 2017. He is currently a Post-Doctoral Fellow with the Centro de Investigaciones en Óptica A. C. His research interests range from optical fiber devices and sensors to light-tissue interaction and image processing.

D. Luna-Moreno received the B.Eng. degree in physics from the Universidad de Guadalajara, Mexico, in 1988, the M.Sc. degree in optics from the Centro de Investigaciones en Óptica A.C., León, México, in 1991, and the Ph.D. degree in optics from the Instituto Nacional de Astrofísica, Óptica y Electrónica, Puebla, México, in 1997. He is currently a Researcher with the Centro de Investigaciones en Óptica A.C. His research interests include design, coating, and characterizations of optical thin films, and optical sensors based on surface plasmon resonance.

M. Torres-Cisneros received the B.Sc. degree in electronics from the Universidad de Guanajuato, México, in 1987, the M.Sc. degree in physics from the Centro de Investigaciones en Óptica A.C., León, México, in 1989, and the Ph.D. degree in physics (nonlinear optics) from the Instituto Nacional de Astrofísica, Optica y Electrónica, Puebla, México, in 1997. He is currently a Researcher with the Electronics Department, University of Guanajuato, Salamanca. His current research interests include optical fiber sensors and their applications.

I. Hernández-Romano received the B.Sc. degree in physics from the Facultad de Ciencias Fisico Matematicas, BUAP, and the M.Sc. and Ph.D. degrees in optics from the Instituto Nacional de Astrofísica, Optica y Electrónica, Puebla, México, in 2007 and 2011, respectively. He is currently a CONACYT Research Fellow with the Electronics Department, University of Guanajuato, Salamanca. His current research interests include optical fiber sensors and their applications.